

# Orbital character of O 2*p* unoccupied states near the Fermi level in CrO<sub>2</sub>

C. B. Stagarescu,<sup>†</sup> X. Su, and D. E. Eastman

*James Franck Institute, The University of Chicago, 5640 South Ellis Avenue, Chicago, Illinois 60637*

K. N. Altmann and F. J. Himpsel

*Department of Physics, University of Wisconsin Madison, 1150 University Avenue, Madison, Wisconsin 53706-1390*

A. Gupta

*IBM T. J. Watson Research Center, Yorktown Heights, New York 10598*

(May 19, 2019; submitted for publication, October 12, 1999)

The orbital character, orientation, and magnetic polarization of the O 2*p* unoccupied states near the Fermi level ( $E_F$ ) in CrO<sub>2</sub> was determined using polarization-dependent X-ray absorption spectroscopy (XAS) and X-ray magnetic circular dichroism (XMCD) from high-quality, single-crystal films. A sharp peak observed just above  $E_F$  is excited only by the electric field vector ( $\mathbf{E}$ ) normal to the tetragonal  $c$ -axis, characteristic of states constituted from O 2*p* orbitals perpendicular to  $c$  (O 2*p<sub>y</sub>*) hybridized with Cr 3*d<sub>xz-yz</sub>*  $t_{2g}$  states. These Cr 3*d*  $t_{2g}$  states have been found to be fully polarized (100% spin-up) by previous electronic structure calculations that predict the half-metallic character of CrO<sub>2</sub>. Consistent with the hybridization with fully polarized empty Cr 3*d* states, the sharp O 2*p* peak exhibits a positive XMCD signal. By comparison with previous calculations our results support a model of CrO<sub>2</sub> as a half-metallic ferromagnet with a large value of the exchange-splitting energy ( $\Delta_{exch-split} \approx 3.2 \pm 0.4$  eV) and substantial correlation effects.

Half-metallic ferromagnets are materials exhibiting metallic character for the majority-spin electrons but a semiconducting gap for the minority-spin electrons.<sup>1</sup> Correspondingly, one expects complete spin polarization at the Fermi level, making this class of materials ideal for spin-polarized emitters to be used in magnetic tunneling applications such as magnetic random access memory<sup>2,3</sup> or spin-polarized scanning tunneling microscopy.<sup>4</sup> Unique among the binary transition metal oxides with the rutile structure, CrO<sub>2</sub> is a ferromagnetic metal with a Curie temperature of  $T_C \approx 390$  K. Recently, it has generated substantial interest<sup>5–11</sup> because its band structure has been predicted to be half-metallic,<sup>6,7,12</sup> which would make it structurally the simplest half-metal. Point contact spectroscopy measurements of a spin polarization of about 90% have been reported recently,<sup>10</sup> providing experimental indication in favor of its half-metallic character.

Since CrO<sub>2</sub> is a metastable phase, it normally has to be synthesized at high oxygen pressures. This has proven to be an impediment for the growth of high-quality films since traditional thin film growth techniques normally operate at atmospheric or lower pressures. However, recent advances<sup>13</sup> made it possible to obtain high-quality, epitaxially grown thin films of CrO<sub>2</sub> by chemical vapor deposition at atmospheric pressure. Samples used in our experiment were as-prepared 4000 Å thick CrO<sub>2</sub> films grown on (100) TiO<sub>2</sub> substrates. X-ray diffraction indicated that the films were single phase and the CrO<sub>2</sub> in-plane  $\langle 100 \rangle$  and  $\langle 001 \rangle$  ( $a_{\parallel}$  and  $c$ ) axes were aligned with the respective axes of the TiO<sub>2</sub> substrate. The third axis, crystallographically equivalent to  $a_{\parallel}$  and normal to the surface of the films, will be denoted as  $a_{\perp}$ . The films exhibited a sharp ferromagnetic transi-

tion with a Curie temperature of about 393 K and a strong in-plane magnetic anisotropy with  $c$  and  $a_{\parallel}$  being the easy-axis and hard-axis directions, respectively. The coercive field ( $H_c$ ) along the easy-axis was of  $\approx 15$  Oe at 5K.<sup>13</sup> Cr<sub>2</sub>O<sub>3</sub> spectra were taken from high-purity pressed-powder samples.<sup>14</sup> Our experiments were performed at the high-resolution Hermon beamline<sup>15</sup> of the University of Wisconsin-Madison Synchrotron Radiation Center. The XAS were taken with a resolution of about 150 meV at 550 eV by measuring the total electron yield. The absolute photon energy calibration was of about  $\pm 100$  meV. The degree of linear polarization was 85-90%. The XMCD measurements were taken with circularly polarized light ( $\approx 80\%$ ) from CrO<sub>2</sub> samples in switching remnant magnetization along the easy-axis which was positioned horizontally and situated at 45° with respect to the direction of the incoming radiation.

To elucidate the spatial orientation and orbital character of the O 2*p* empty states we have employed polarization-dependent XAS measurements with linearly polarized light. The results are shown in Fig. 1(a) where we plot O  $K$  XAS spectra taken in a geometry with fixed polar angle between the  $c$ -axis and the photon direction ( $\theta=90^\circ$ ) and variable azimuthal angle ( $\phi$ ) between the polarization direction and  $a_{\parallel}$ . The CrO<sub>2</sub> spectrum displays a sharp peak (1) at  $\approx 529.2$  eV, followed by two other features (2) and (3) at energies of 2.3 and 3.4 eV higher. The sharp peak (1) exhibits a large intensity variation of  $\approx 90\%$ , with a maximum for the geometry with the electric field vector of the light  $\mathbf{E}$  arranged along  $a_{\parallel}$  and normal to the  $c$ -axis. As shown further in Fig. 1(b), the  $\phi$  dependence of (1) follows accurately a  $\cos^2(\phi)$  curve. Our fit to the data, together with the degree of linear polarization of 85-90%, gives an

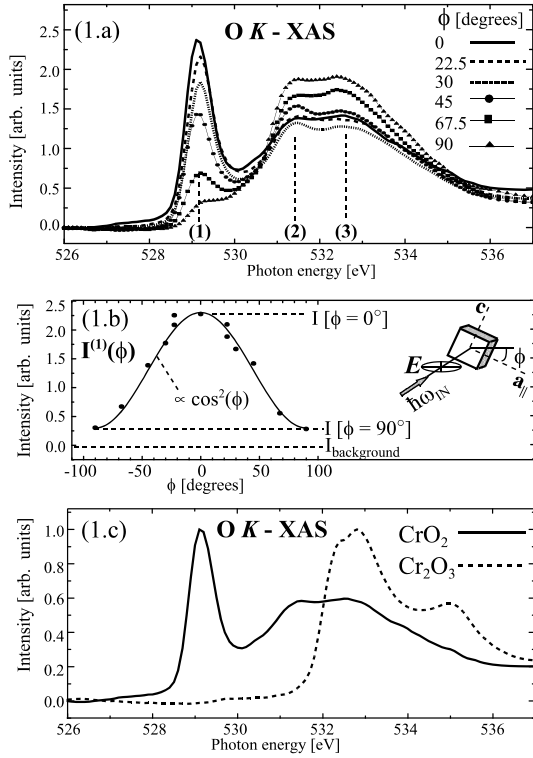


FIG. 1. (a). O  $K$  XAS of  $\text{CrO}_2$  taken in a geometry with fixed polar angle between the  $c$  axis and the photon direction ( $\theta=90^\circ$ ) and variable azimuthal angle ( $\phi$ ) between the photon direction and  $a_{\parallel}$ . (b). Intensity variation of the peak (1) with the azimuthal angle  $\phi$ . The experimental geometry is shown in the inset. (c). Comparison of the O  $K$  XAS of  $\text{CrO}_2$  and  $\text{Cr}_2\text{O}_3$ .

orientation of peak (1) perpendicular to the  $c$ -axis of more than 95%.<sup>16</sup> The azimuthal dependence of the higher lying features (2) and (3) is considerably smaller exhibiting an excursion of about 28% between the  $0^\circ$  and  $90^\circ$  orientations. At the same time its sign is opposite to that of (1) which indicates a dominant contribution from O  $2p$  states parallel to the  $c$ -axis.

In order to analyze the origin of the O  $K$  XAS polarization dependence it is useful to understand the bonding configuration and directionality of the O  $2p$  - Cr  $3d$  hybrid states with respect to the crystalline axes.  $\text{CrO}_2$  crystallizes in the rutile structure which has a simple tetragonal Bravais lattice with two formula units per unit cell. The building blocks of this structure are  $\text{CrO}_6$  octahedra arranged along and slightly elongated in the direction of the tetragonal  $c$  axis. The O  $2p$  - Cr  $3d$  hybridization mechanism can be easily understood in a Goodenough molecular-orbital model electronic structure scheme.<sup>17-20</sup> Inside each of the  $\text{CrO}_6$  octahedra the crystal-field splits the Cr  $3d$  manifold into three  $t_{2g}$  and two  $e_g$  states. Due to the distinction between the  $a_{\perp}$  ( $a_{\parallel}$ ) and the  $c$ -axes in the tetragonal rutile structure the  $t_{2g}$  group of Cr  $3d$  states undergoes a further, small degeneracy splitting into an orbital normal to the  $c$ -axis ( $d_{xz-yz}$ )

and two other having non-zero  $c$ -axis projections ( $d_{xz+yz}$  and  $d_{xy}$ ). Oxygen atoms are situated in a trigonal environment forming planar  $\text{CrO}_3$  clusters with the three closest Cr atoms, with the planes of these  $\text{CrO}_3$  clusters running parallel to the  $c$  axis and oriented at  $45^\circ$  with respect to the  $a_{\parallel}$  and  $a_{\perp}$  directions. This trigonal ligand environment of oxygen leads to two  $sp^2$  combinations (O  $2s$  and  $2p_{x,y}$ ) with non-zero  $c$ -axis projections situated in the planes of the  $\text{CrO}_3$  clusters and one remaining  $p$  state (O  $2p_y$ ) that resides in the  $a_{\parallel}$ - $a_{\perp}$  planes. The Cr  $d_{xz-yz}$  states are therefore properly oriented to lead to  $\pi$ -type bonding with the O  $2p$  available orbital which is perpendicular to the  $c$ -axis, i.e., O  $2p_y$ . The remaining two oxygen orbitals, O  $2p_{x,z}$ , yield  $\sigma$ -type combinations with the Cr  $3d e_g$  states. Thus, the preceding analysis of the peak's (1) polarization dependence allows us to clearly identify it with empty states normal to the tetragonal  $c$ -axis formed by O  $2p_y$  hybridized with Cr  $3d_{xz-yz}$ . This result is confirmed by recent band-structure calculations (LSDA+U) of  $\text{CrO}_2$  which find that in the first  $\approx 2$  eV above  $E_F$  the empty O  $2p$  states are 100% oriented perpendicular to the  $c$ -axis.<sup>21</sup>

It should be noted that even under normal pressure/temperature conditions  $\text{CrO}_2$  ( $\text{Cr}^{4+}$ ) undergoes a chemical reduction to  $\text{Cr}_2\text{O}_3$  ( $\text{Cr}^{3+}$ ) which is the stable oxidation state of Cr. For our samples, we estimated by tunneling measurements a  $\text{Cr}_2\text{O}_3$  surface layer thickness of about 10 Å. We have addressed the issue of spectral contamination effects of the native insulating surface layer by measuring O  $K$  XAS from  $\text{Cr}_2\text{O}_3$  on the same experimental setup. The results are shown in Fig. 1(c). In contrast to  $\text{CrO}_2$ , the  $\text{Cr}_2\text{O}_3$  O  $K$  XAS spectrum displays significant intensity only above 532 eV having the highest intensity at about 532.8 eV. Therefore we can conclude that the energy region from 529 to about 532 eV in our  $\text{CrO}_2$  O  $K$  XAS does not contain any spectral interference from the surface layer of  $\text{Cr}_2\text{O}_3$ .

Our  $\text{CrO}_2$  O  $K$  XAS spectra (peak (1) at 529.2 eV) have been taken with a resolution of 150 meV and an accuracy of the absolute photon energy scale of about  $\pm 100$  meV. Previously reported O  $K$  absorption energies for peak (1) taken from powder  $\text{CrO}_2$  are of 527.0 eV<sup>11</sup>, 530.0 eV<sup>22</sup>, and  $\approx 530.5$  eV<sup>9</sup>. Our experience with measuring the  $\text{CrO}_2$  and  $\text{Cr}_2\text{O}_3$  absorption spectra suggests that these differences are due to monochromator absolute energy calibration errors rather than to sample differences.<sup>22</sup> O  $1s$  binding energies ( $E_B$ ) measurements using x-ray photoelectron spectroscopy have been previously reported for  $\text{CrO}_2$ <sup>23</sup> and  $\text{Cr}_2\text{O}_3$ <sup>23,24</sup>. The  $\text{CrO}_2$  O  $1s$  binding energy<sup>23</sup> ( $E_B = 529.3$  eV) is within 0.1 eV of the absorption peak (1) transition which is within the typical accuracy of these XPS measurements of  $\leq 0.1$ - $0.2$  eV. Thus, we can conclude that the XAS final-state excitonic effects are not large in  $\text{CrO}_2$  and peak (1) represents the lowest group of empty O  $2p$  states situated within  $\leq 400$  meV of  $E_F$ .

Further understanding of the electronic structure of

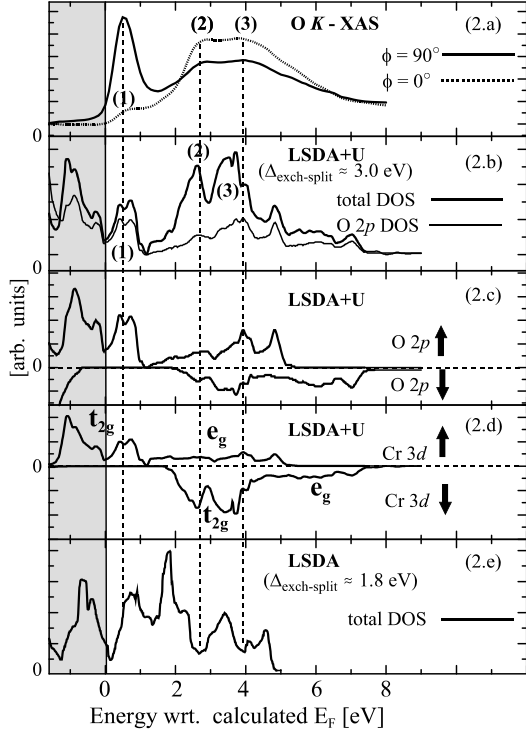


FIG. 2. Comparison of the  $\text{CrO}_2$  O  $K$  XAS with calculated DOS from two recent calculations.<sup>6,7</sup> The theoretical DOS are plotted against their calculated binding energy scales. The sharp XAS peak (1) is aligned to the isolated set of states (1) in the calculated DOS. Since the spectral shapes and not the absolute intensities are of interest in this comparison, the theoretical curves have been scaled for visibility and only the zero intensity position is indicated in each of the panels. (a).  $\text{CrO}_2$  O  $K$  XAS for two azimuthal angles  $\phi = 0^\circ$  and  $90^\circ$ . (b). Total DOS and O  $2p$  partial DOS from the LSDA+U calculation of Korotin *et al.*<sup>6</sup> (c, d). O  $2p$  and Cr  $3d$  spin resolved DOS from the same LSDA+U work<sup>6</sup>. Labels  $t_{2g}$  and  $e_g$  mark the approximative "centers of mass" of the respective components of the Cr  $3d$  manifold for each spin orientation. (e). Total DOS from the LSDA calculation of Lewis *et al.*<sup>7</sup>

$\text{CrO}_2$  will be gained by the means of a comparison with results of two recent band-structure calculations.<sup>6,7</sup> The two calculations used in this study<sup>6,7</sup> are both ground-state, band-structure calculations based on the local-spin-density approximation of the density-functional theory (LSDA). In the traditional LSDA approach of Lewis *et al.*<sup>7</sup> the effects of electron-electron correlation are included in an averaged, mean-field way. In contrast, Korotin *et al.*<sup>6</sup> use a LSDA scheme modified by the explicit inclusion of a potential correction in order to account for the Coulomb interaction between localized  $d$  electrons. In the resulting LSDA+U scheme a substantial Coulomb on-site correlation energy ( $U=3\text{eV}$ ) was used in order to account properly for the half-metallic character of  $\text{CrO}_2$ . Both calculations find  $\text{CrO}_2$  to be a half-metal but differ importantly in the values obtained

for the exchange-splitting energy responsible for ferromagnetism. The general characteristics of the electronic structure of  $\text{CrO}_2$  are best understood by investigating the density of states (DOS) of dominant Cr  $3d$  states resolved in spin-up and spin-down components (Fig. 2(d)). The Cr  $3d$   $t_{2g}$  spin-up part is almost split, displaying a deep valley with low DOS at  $E_F$ . This leaves the first 1.5 eV above  $E_F$  to be of fully spin-up character and dominated by a structure centered at about 0.6 eV. As observed for the LSDA+U calculation, the DOS of the relatively delocalized unoccupied O  $2p$  states (Fig. 2(c)) are found to follow very closely their corresponding Cr  $3d$  spin-up/spin-down curves which is expected for states strongly mixed by hybridization. As an immediate result (Fig. 2(b)) the spin-summed O  $2p$  DOS has a very similar overall shape to the total DOS. We find a good similarity between the O  $K$  XAS and the envelope of the O  $2p$  unoccupied DOS obtained in the LSDA+U scheme of Korotin *et al.*, as can be observed by comparing spectra in panels (a) and (b) of Fig. 2. In particular, the sharp XAS peak (1) (Fig. 2(a)) at 529.2 eV is of comparable width<sup>25</sup> to the set (1) (Fig. 2(b)) of unoccupied O  $2p$  states that in turn follow closely the envelope of the empty, isolated Cr  $3d$   $t_{2g}$  spin-up DOS. The two other O  $K$  XAS features, (2) and (3) at higher energies, correspond to local DOS maxima that have a mixed O  $2p$  - Cr  $3d$   $e_g$  spin-up and O  $2p$  - Cr  $3d$   $t_{2g}$  spin-down character. It becomes clear when looking at the theoretical spin-up/spin-down projected DOS in Fig. 2(c) and 2(d) that in order to obtain the broad minimum in the empty DOS at  $\approx 1.5$  eV above  $E_F$  and the large local maxima (2) and (3) at higher energies, as observed experimentally, a considerable upward energy shift ( $\Delta_{\text{exch-split}}$ ) of the spin-down component must be considered. Our data are not well reproduced by the LSDA calculation<sup>7</sup> which yields  $\Delta_{\text{exch-split}} \approx 1.8$  eV. Instead, the agreement is consistent with the LSDA+U work<sup>6</sup> which has  $\Delta_{\text{exch-split}} \approx 3.0$  eV, as measured between the "centers of mass" of the Cr  $3d$   $t_{2g}$  spin-up and spin-down DOS distributions (Fig. 2(d)). An experimental  $\Delta_{\text{exch-split}}$  can be determined in a "rigid band" approximation by slightly adjusting the upward exchange-splitting energy shift to fit our data (features (2) and (3)). This fit (taking into account also the limited accuracies present in the absolute photon energies and O  $1s$  binding energy determination) yields  $\Delta_{\text{exch-split}} \approx 3.2 \pm 0.4$  eV. This rather large upward energy shift of the unoccupied  $d$  spin-down states was obtained in the LSDA+U work<sup>6</sup> as an explicit consequence of the inclusion of a considerable correlation energy ( $U=3\text{eV}$ ). Thus, our experimental results add support for the presence of important on-site correlation effects in  $\text{CrO}_2$ .

A final test that our analysis must pass refers to the ferromagnetism of  $\text{CrO}_2$ . Indeed, as the first ligand empty states have been experimentally determined to be of O  $2p_y$  origin, a substantial orbital polarization of these states is expected since their Cr  $3d_{xz-yz}$   $t_{2g}$  counterparts are fully spin-polarized (Fig. 2(d)).

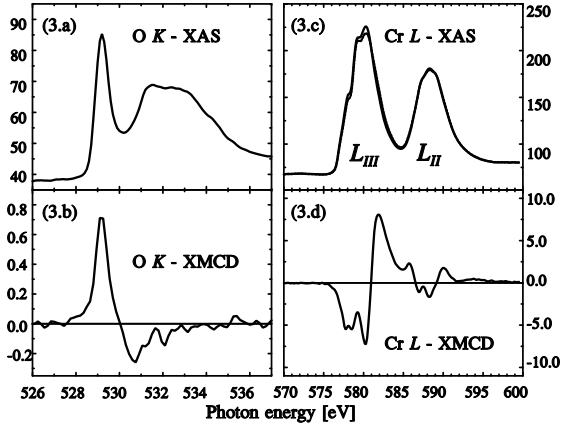


FIG. 3. CrO<sub>2</sub> XAS and XMCD at the O *K* and Cr *L* edges.

This ligand orbital polarization is clearly exhibited in Fig. 3(b) which shows the presence of a positive O *K* XMCD difference signal. Our O *K* XMCD is similar to that obtained previously by Attenkofer *et al.*<sup>8</sup> from polycrystalline CrO<sub>2</sub>.

In conclusion, we used polarization-dependent XAS to determine the orbital character of the unoccupied O *2p* states just above  $E_F$  in CrO<sub>2</sub> which are found to be O *2p<sub>y</sub>* states hybridized with Cr *3d<sub>xz-yz</sub>* *t<sub>2g</sub>*. This hybridization with fully polarized Cr *3d* *t<sub>2g</sub>* states implies a substantial ligand orbital polarization which was proven experimentally by the existence of a positive O *K* XMCD signal. The exchange-splitting energy was found to be a sensitive and important parameter in establishing agreement between our data and recent band-structure calculations. An experimental exchange-splitting energy of  $\Delta_{exch-split} \approx 3.2 \pm 0.4$  eV was determined. Our results support a model of CrO<sub>2</sub> as a half-metallic ferromagnet with substantial correlation effects, consistent with the LSDA+U band-structure calculations of Korotin *et al.*<sup>6</sup>

The authors thank M. A. Korotin for communicating his results prior to publication. One of the authors (C. B. S.) thanks G. A. Sawatzky and D. I. Khomskii for useful discussions. The help of M. Bissen and R. Hansen is gratefully acknowledged. This work was supported in part by the DOE under Contract W-31-109-ENG-38. The Synchrotron Radiation Center, UW-Madison, is supported by the NSF under Award No. DMR-9531009.

<sup>†</sup> Author to whom correspondence should be addressed (electronic mail: c-stagarescu@uchicago.edu).

<sup>1</sup> R. A. de Groot, F. M. Mueller, P. G. van-Engen-PG, and K. H. J. Buschow, *Half-metallic ferromagnets and their magneto-optical properties*, Phys. Rev. Lett. **50**, 2024

(1983).

- <sup>2</sup> W. J. Gallagher, S. S. P. Parkin, Yu Lu, X. P. Bian, A. Marley, R. A. Altman, S. A. Rishton, K. P. Roche, C. Jahnes, T. M. Shaw, and Xiao Gang, *Microstructured magnetic tunnel junctions*, J. Appl. Phys. **81**, 3741 (1997).
- <sup>3</sup> J. M. Daughton, *Magnetic tunneling applied to memory (invited)*, J. Appl. Phys. **81**, 3758 (1997).
- <sup>4</sup> R. Wiesendanger, H. J. Güntherodt, G. Güntherodt, R. J. Gambino, and R. Ruf, *Observation of vacuum tunneling of spin-polarized electrons with the scanning tunneling microscope*, Phys. Rev. Lett. **65**, 247 (1990).
- <sup>5</sup> J. M. D. Coey *et al.*, A. E. Berkowitz, Ll. Balcells, F. F. Putris, and A. Barry, *Magnetoresistance of Chromium Dioxide Powder Compacts*, Phys. Rev. Lett. **80**, 3815 (1998); H. Y. Hwang and S. -W. Cheong, *Enhanced intergrain tunneling magnetoresistance in half-metallic CrO<sub>2</sub> films*, Science **278**, 1607 (1997); I. I. Mazin, D. J. Singh, and C. Ambrosch-Draxl, *Transport, optical, and electronic properties of the half-metal CrO<sub>2</sub>*, Phys. Rev. B **59**, 411 (1999); R. J. Soulen, J. M. Byers, M. S. Osofsky, B. Nadgorny, T. Ambrose, S. F. Cheng, P. R. Broussard, C. T. Tanaka, J. Nowak, J. S. Moodera, A. Barry, and J. M. D. Coey, *Measuring the spin polarization of a metal with a superconducting point contact*, Science **282**, 85 (1997).
- <sup>6</sup> M. A. Korotin, V. I. Anisimov, D. I. Khomskii, and G. A. Sawatzky, *CrO<sub>2</sub> a self-doped double exchange ferromagnet*, Phys. Rev. Lett. **80**, 4305 (1998).
- <sup>7</sup> S. P. Lewis, P. B. Allen, and T. Sasaki, *Band structure and transport properties of CrO<sub>2</sub>*, Phys. Rev. B **55**, 10253 (1997).
- <sup>8</sup> K. Attenkofer and G. Schütz, *Hard and Soft X-MCD Studies of CrO<sub>2</sub>*, J. Phys. IV France **7**, C2-459 (1997).
- <sup>9</sup> D. Ahlers, K. Attenkofer, and G. Schütz, *Spin-dependent extended X-ray absorption fine structure in magnetic oxides*, J. Appl. Phys. **83**, 7085 (1998).
- <sup>10</sup> R. J. Soulen, J. M. Byers, M. S. Osofsky, B. Nadgorny, T. Ambrose, S. F. Cheng, P. R. Broussard, C. T. Tanaka, J. Nowak, J. S. Moodera, A. Barry, and J. M. D. Coey, *Measuring the spin polarization of a metal with a superconducting point contact*, Science **282**, 85 (1997).
- <sup>11</sup> T. Tsujioka, T. Mikoza, J. Okamoto, and A. Fujimori, *Hubbard splitting and electron correlation in the ferromagnetic metal CrO<sub>2</sub>*, Phys. Rev. B **56**, R15509 (1997).
- <sup>12</sup> K. Schwarz, *CrO<sub>2</sub> predicted as a half-metallic ferromagnet*, J. Phys. F **16**, L211 (1986).
- <sup>13</sup> X. W. Li, A. Gupta, and G. Xiao, *Influence of strain on the magnetic properties of epitaxial (100) chromium dioxide (CrO<sub>2</sub>) films*, Appl. Phys. Lett. **75**, 713 (1999); X. W. Li, A. Gupta, T. R. McGuire, P. R. Duncombe, and Gang Xiao, *Magnetoresistance and Hall effect of chromium dioxide epitaxial thin films*, J. Appl. Phys. **85**, 5585 (1999).
- <sup>14</sup> Alfa Aesar, Chromium(III) oxide, 99%.
- <sup>15</sup> M. Bissen, M. Fisher, G. Rogers, D. Eisert, K. Kleman, T. Nelson, B. Mason, F. Middleton, and H. Hachst, *First results of SRC's new high-energy resolution variable line density grating monochromator beamline: HERMON*, Rev. Sci. Instrum. **66**, 2072 (1995). We have taken a few spectra with a better resolution ( $\approx 50$  meV at 550 eV) but no additional structure could be resolved.
- <sup>16</sup> In the dipole approximation which can be safely employed

at these energies, the rate of the absorption process is proportional to  $\langle f|\mathbf{E}\cdot\mathbf{p}|i\rangle$ , where  $\mathbf{p}$  is the linear momentum operator of the electron,  $\mathbf{E}$  the electrical vector of the photon field, and  $|i\rangle$ ,  $|f\rangle$  denote the initial and final states (J. Stöhr, NEXAFS Spectroscopy, Springer (1996)). Label  $\mathbf{E}$  used in text denotes the dominant, horizontal component ( $\mathbf{E}_{\parallel}$ ) of the electrical vector. Due to the incomplete linear polarization (85-90%) a small, vertical component ( $\mathbf{E}_{\perp}$ ) was also present which accounts to within 5% for the leftover intensity of peak (1) at  $\phi=90^{\circ}$ .

- <sup>17</sup> P. I. Sorantin and K. Schwarz, *Chemical Bonding in Rutile-Type Compounds*, Inorg. Chem. **31**, 567 (1992). Note that the  $x, y, z$  subscripts attached to the  $d$  and  $p$  orbitals denote local coordinates in the  $\text{CrO}_6$  octahedra and not the crystalline directions.
- <sup>18</sup> J. B. Goodenough, *Metallic Oxides*, in Prog. Sol. State Chem. **5**, 145 (1971).
- <sup>19</sup> D. S. Chapin, J. A. Kalafas and J. M. Honig, J. Phys. Chem. **69**, 1402 (1965).
- <sup>20</sup> B. L. Chamberland, *The chemical and physical properties of  $\text{CrO}_2$  and tetravalent chromium oxide derivatives*, CRC

Crit. Rev. Sol. State Mat. Sci. **7**, 1 (1977).

- <sup>21</sup> M. A. Korotin *et al.* (unpublished) and G.A. Sawatzky (private communication).
- <sup>22</sup> Th. Schedel-Niedrig, Th. Neisius, C. T. Simmons, and K. Köhler, *X-ray absorption spectroscopy of small chromium oxide particles ( $\text{Cr}_2\text{O}_3$ ,  $\text{CrO}_2$ ) supported on titanium oxide*, Langmuir **12**, 6377 (1996). The energy separation determined in this work between the  $\text{CrO}_2$  peak (1) and the highest feature of the  $\text{Cr}_2\text{O}_3$  XAS is very close to our value ( $\approx 3.6$  eV).
- <sup>23</sup> I. Ikemoto, S. Kinoshita, H. Kuroda, K. Ishii, M. A. Alario-Franco, and J. M. Thomas, *X-ray photoelectron spectroscopic studies of  $\text{CrO}_2$  and some related chromium compounds*, J. Solid State Chem. **17**, 425 (1976).
- <sup>24</sup> M. Hassel, I. Hemmerich, H. Kuhlenbeck, and H.-J. Freund, *High-resolution XPS study of a thin  $\text{Cr}_2\text{O}_3$  film grown on  $\text{Cr}(110)$* , Surf. Sci. Spectra **4**, 246 (1998).
- <sup>25</sup> The experimental width is slightly larger due to additional broadening effects of the finite excitation bandpass and finite lifetime of the excited XAS final state.